Solar Phys (2008) 252: 283–292
DOI 10.1007/s11207-008-9271-z

EIS/*Hinode* Observations of Doppler Flow Seen through the 40-Arcsec Wide-Slit

D.E. Innes · R. Attie · H. Hara · M.S. Madjarska

Received: 19 March 2008 / Accepted: 10 September 2008 / Published online: 10 October 2008

Abstract The Extreme ultraviolet Imaging Spectrometer (EIS) onboard *Hinode* is the first solar telescope to obtain wide-slit spectral images that can be used for detecting Doppler flows in transition region and coronal lines on the Sun and to relate them to their surrounding small-scale dynamics. We select EIS lines covering the temperature range 6×10^4 to 2×10^6 K that give spectrally pure images of the Sun with the 40-arcsec slit. In these images Doppler shifts are seen as horizontal brightenings. Inside the image it is difficult to distinguish shifts from horizontal structures but emission beyond the image edge can be unambiguously identified as a line shift in several lines separated from others on their blue or red side by more than the width of the spectrometer slit (40 pixels). In the blue wing of He II, we find a large number of events with properties (size and lifetime) similar to the well-studied explosive events seen in the ultraviolet spectral range. Comparison with X-Ray Telescope (XRT) images shows many Doppler shift events at the footpoints of small X-ray loops. The most spectacular event observed showed a strong blue shift in the transition region and lower corona lines from a small X-ray spot that lasted less than 7 min. The emission appears to be near a cool coronal loop connecting an X-ray bright point to an adjacent region of quiet Sun. The width of the emission implies a line-of-sight velocity of 220 km s^{-1}. In addition, we show an example of an Fe XV shift with a velocity of about 120 km s^{-1}, coming from what looks like a narrow loop leg connecting a small X-ray brightening to a larger region of X-ray emission.

Keywords Corona: quiet · Jets · Transition region

D.E. Innes (✉) · R. Attie · M.S. Madjarska
Max-Planck Institut für Sonnensystemforschung, 37191 Katlenburg-Lindau, Germany
e-mail: innes@mps.mpg.de

H. Hara
National Astronomical Observatory, Mitaka, Tokyo 181-8588, Japan

1. Introduction

The Extreme ultraviolet Imaging Spectrometer (EIS; Culhane *et al.*, 2007) on *Hinode* obtains images and spectra of many transition region and coronal lines in the wavelength ranges 170 – 211 Å and 246 – 292 Å. The EIS wide slits are an interesting compromise between narrow-slit spectra where the time to raster across a particular structure is often longer than the lifetime of the structure and filter images, which give no direct measurement of flow velocities. The 40-arcsec wide-slit provides overlapping spectra from the observed 40-arcsec region of the Sun. Images in different lines overlap if the lines are separated by less than the 40-pixel width of the slit image times the wavelength plate scale, 0.0223 Å/pixel. Figure 1 shows a 40-arcsec wide-slit spectrum of a small active region for the wavelength region 268 – 292 Å. Isolated lines produce well-defined 40-arcsec images.

Within the EIS spectrum there are several relatively strong isolated lines that can be used to study the dynamics of the outer atmosphere. Hansteen *et al.* (2007) report on rapid temporal variations in quiet Sun He II 256 Å and Fe XII 195 Å wide-slit emission features observed with a cadence of 30 s. They also mention the detection of many He II blue shifts in quiet Sun narrow-slit rasters observed after the wide-slit sequence.

In this paper we show how the detection of He II blue shifts and large-scale temporal variations can be made simultaneously with wide-slit observations. The key is that the emission beyond the edge of the 40-arcsec main line image is either line broadening/Doppler shifts from the main line or emission in a neighboring line. Figure 1 demonstrates both effects. Fe XV and Fe XIV (labeled) are both well-separated lines and the images are basically straight along both edges. On the edge that cuts the active region, the emission from both lines bulges slightly because the bright active region lines are broader. A closer inspection of the emission shows that both lines have the same structure along the edge. However, the strong unmarked line on the left is mainly Fe XIV 270.5 Å, but there is clearly a blend producing extensions on the left-hand side. Positions of the projections coincide with bright Mg VII and Si VII because the blend is the lower coronal line Mg VI 270.4 Å.

When the Sun's structure is known from images in isolated lines, it is possible to work out from the spectrum whether neighboring lines are expected to produce emission. If there is no spectral line that can cause the emission, it is very likely due to Doppler shifts/broadening in the image line. Thus the EIS 40-arcsec wide-slit can be used to obtain both images of the dynamics over a wide range of temperatures and Doppler shifts from structures on the edge of the images.

Inside the image, Doppler-broadened lines appear as horizontal streaks, which are difficult to distinguish from a jetlike structure. Comparison with filter images is very important for positively identifying shifts inside the image. Simultaneous images obtained by other instruments on *Hinode* can, in principle, be used to help identify shifts but there will always be some uncertainty because the filters do not detect exactly the same plasma.

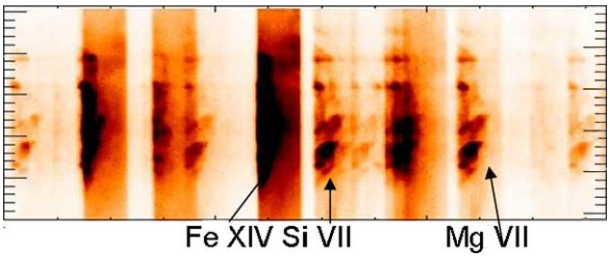

Figure 1 A 40-arcsec wide-slit spectrum of a small active region, showing well-separated and blended lines. Several of the lines discussed in this paper are marked.

In this paper we show examples of Doppler shift events seen in the quiet Sun with the EIS 40-arcsec wide-slit. Comparisons are made with X-ray images obtained by the X-Ray Telescope (XRT; Golub *et al.*, 2007) to show the relationship to hot loop structures. Further work will report on detailed analyses with data from the Solar Optical Telescope (SOT; Tsuneta *et al.*, 2008) on *Hinode* and the Solar Ultraviolet Measurements of Emitted Radiation (SUMER; Wilhelm *et al.*, 1995) spectrograph on SOHO.

2. Observations

Observations are shown of regions of quiet Sun near disk center on 10 April 2007 and 7 November 2007, and near a small active region on 15 November 2007. During the April observations, EIS observed with the 40-arcsec slit and a cadence of 30 s at a single position. During the November runs EIS alternated between two slit positions separated by 40 arcsec with an exposure time of 30 s and cadence of 90 s. In April, windows centered on the lines given in Table 1 were recorded. To keep within the telemetry rate, JPEG lossy compression ($Q = 98$) was used. In November only the ones marked with an asterisk in Table 1 were recorded and lossless compression was used. For all observations the window height was 512 arcsec and for most lines the window width was 56 wavelength pixels. The windows around the EIS core lines He II, Fe XII, and Fe XV were 64 pixels wide to ensure at least 8 pixels either side of the image.

The 80-pixel spectral regions around nine of the strongest isolated lines are shown in Figure 2. The cleanest line is Fe XIV 274.20 Å. The two lines He II 256.32 Å and Si VII 275.35 Å are clean on their blue side. The lines Fe XV 284.25 Å and Fe XIII 203.86 Å are clean for more than 15×0.0223 Å or 400 km s^{-1} to one or both sides. These lines are suitable for obtaining Doppler shifts at the edge of the 40-arcsec images. The Si X 272.01 Å line appears unblended in Figure 2, but it is known to be blended with several transition region lines (Young *et al.*, 2007a), so is only useful as a check on what one sees in other lines.

To assess this method of measuring velocities, we constructed pseudo-wide-slit images from rasters of 2-arcsec slit observations. Line profiles with significant extensions two pixels from the line center could be identified as Doppler shifts at the window edge. This corresponds to 52 km s^{-1} at He II 256 Å and 48 km s^{-1} at Fe XV 284 Å.

Table 1 Spectral lines in the center of each window during the 10 April 2007 observations. The entries in bold are illustrated in Figure 2. Those with an asterisk are separated from other strong lines and produce spectrally pure images. They were observed in November 2007.

Ion	Wavelengths			Log T (K)
He II	**256.32***			4.7
Mg VII	**278.39***	280.75		5.8
Si VII	**275.35***			5.8
Fe X	184.54	190.04		6.0
Si X	258.37*	**261.08***	**272.01***	6.1
Fe XI	180.40*	188.25		6.1
Fe XII	**195.12***			6.1
Fe XIII	202.08	**203.86***		6.2
Fe XIV	264.88	**274.20***		6.3
Fe XV	**284**.16*			6.3
Fe XVI	263.02*			6.4
Ca XVII	192.82			6.7

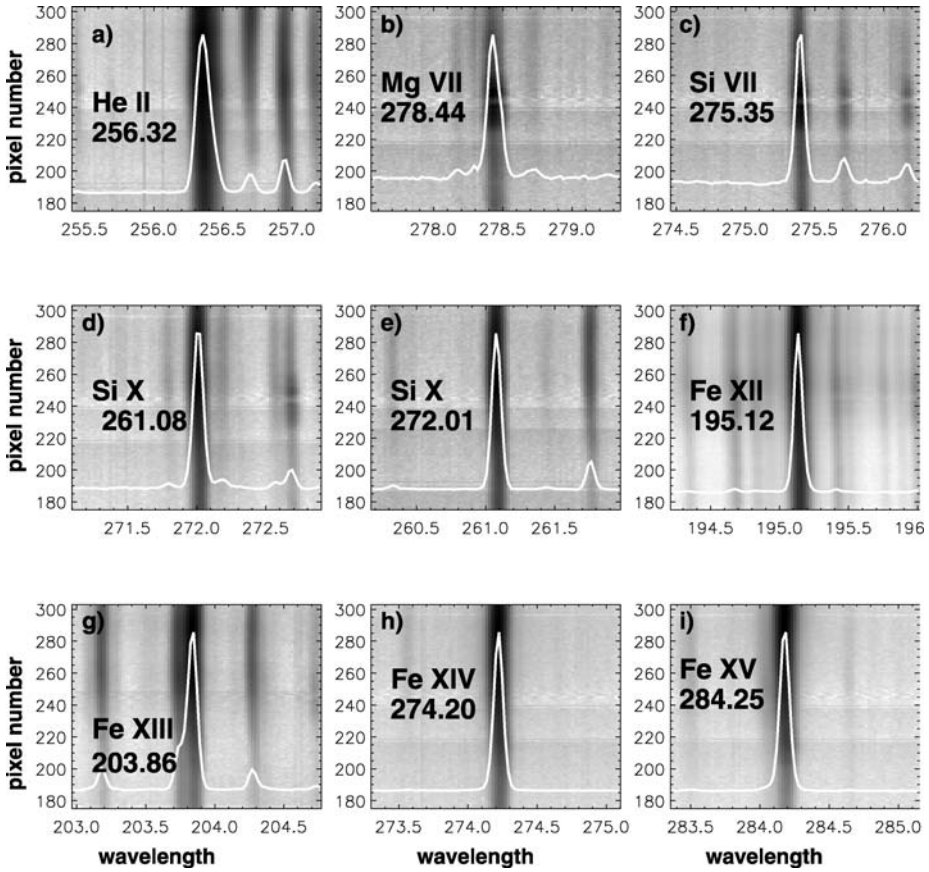

Figure 2 80-pixel spectral region around selected strong isolated lines giving the purest 40-arcsec slit images. The background of each frame is a stigmatic spectral image taken with the 2-arcsec slit across a small active region on 3 April 2007. The images are negatives and bright lines appear dark. Higher temperature lines are stronger at the top of the images. Superimposed are the average line profiles along the length of the slit.

The EIS images suffer from misalignment owing to spacecraft jitter and internal drift from EIS temperature changes. The former changes the field of view, and the latter shifts the image on the CCD. The instrument movement owing to spacecraft jitter in the Sun-x (spectral) and Sun-y directions was corrected by first coaligning all images in a particular spectral window to the average for that window. This was done to assess the best window for obtaining the instrumental shifts. The He II, Si VII, and Mg VII coalignment parameters were similar and appeared to successfully remove the instrument movement. Therefore these were applied to all images in the same sequence. The maximum shift is 1.5 pixels in the Sun-y direction and less than 1 pixel in the Sun-x direction. To investigate emission just beyond the window edge, the movement of the window edge rather than of the solar features was taken into account. Over a typical one-hour observing period the window edge drifted less than 1 pixel on the detector. It is important to note therefore that images used for computing the Doppler shifts beyond the edge have a slightly different coalignment than those that show the structural changes.

In this paper, the EIS wide-slit images are presented such that the Sun-y coordinate increases toward the top and the Sun-x coordinate increases to the right of the images. The wavelength scale then decreases to the right, so that blue shifts are seen beyond the right edge of the images.

Simultaneous XRT images were obtained in April with the Al-mesh filter and a cadence of 20 s and in November with the C-poly filter and a cadence of 30 s. The data were corrected by using the standard SOLARSOFT XRT software. Coalignment of the EIS and XRT images was achieved by cross-correlating common Fe XV and X-ray features.

3. Dynamics

3.1. He II Explosive Events

Explosive events are characterized by Doppler-broadened line wings in transition region lines. They have been well studied with HRTS (Brueckner and Bartoe, 1983; Dere, Bartoe, and Brueckner, 1989) and SUMER (Innes *et al.*, 1997a, 1997b; Chae *et al.*, 1998; Ning, Innes, and Solanki, 2004) ultraviolet spectra. In the quiet Sun, most strong events are seen in lines formed in the transition region with formation temperature of 6×10^4 to 3×10^5 K (Winebarger *et al.*, 2002). In active regions strong explosive events have also been reported in lower corona lines such as Ne VIII with formation temperature of around 7×10^5 K (Wilhelm *et al.*, 1998).

There are several transition region and lower corona lines in the EIS wavelength range (Young *et al.*, 2007b). The three lines He II 256.32 Å, Mg VII 278.39 Å, and Si VII 275.35 Å all give sharp wide-slit images. He II is ideal for detecting explosive events at the image edge because it is formed around 6×10^4 K and there are no lines on its blue side that will overlap with the Doppler-shifted emission. The red side of the He II line is blended and overlaps with images produced by the strong coronal lines Si X 256.37 Å, Fe XIII 256.42 Å, Fe XII 256.41 Å, and Fe XII 256.94 Å, so He II blue shifts are more easily detectable. The best line for shifts in the lower corona is Si VII 275.35 Å. It is clean on the blue side and for 14 pixels to the red where there is a second, weaker Si VII line. The Mg VII 278.39 Å line shows blending with coronal lines in Figure 2 and is known to be blended with Si VII (Young *et al.*, 2007b), so it may not always be easy to interpret in wide-slit images.

Figure 3 demonstrates the method used to enhance blue shifts in He II at the edge of the image. Here images from a region of quiet Sun in Fe XII (a) and He II (b – d) are shown. There is no structure in the Fe XII image but the He II image (b) shows the outline of supergranular cells. To bring out the brightening on the west edge (blue wing) the logarithm of intensity is shown in (c); in (d) the image is divided by the average He II image for the one-hour period of observation. At this time there were three explosive events around Sun $x = -70$, -45, and -20 arcsec. It is not possible to determine the Doppler velocity precisely because these are not real line profiles. We estimate that they are of the order of a couple of pixels, or 60 km s^{-1}. Another advantage of dividing by the average for the observing period is that brightenings in the image would also show up and warn that edge brightenings may be due to a neighboring line brightening in a structure inside the image. This is not the case for the three events identified.

The advantage of the wide slit is that it shows the structure surrounding these Doppler-shift events. We have therefore combined the He II, Fe XII, and Fe XV wide-slit images with the Doppler-shift information in a short movie, showing one hour of quiet Sun observations. One frame from the movie is shown in Figure 4. During the observing sequence two

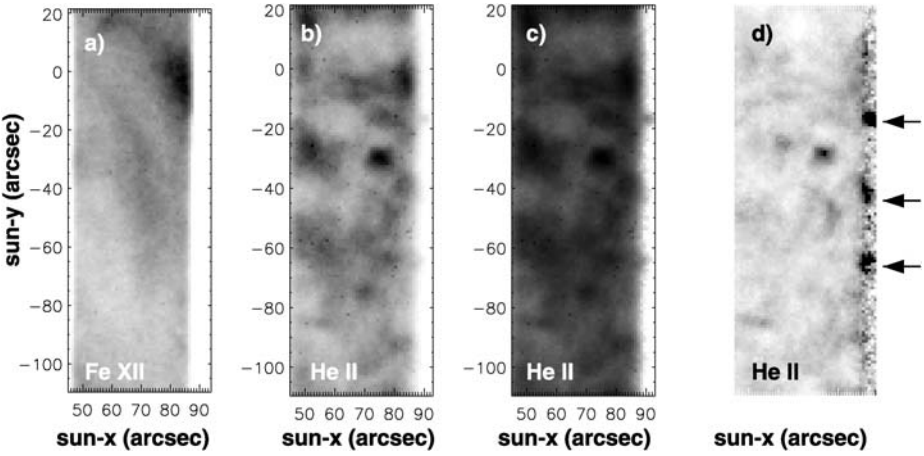

Figure 3 Explosive events seen in He II in the quiet Sun images taken at 21:45:57 UT on 10 April 2007 in Fe XII 195 Å and He II 256 Å (as labeled). The He II images are scaled (b) linearly, (c) logarithmically and (d) relative to the average for the one-hour observation period. The three explosive events, indicated with arrows and seen on the right of the He II frames, are blue shifts because the spectral images have been flipped so that west is on the right. All images are shown as negatives.

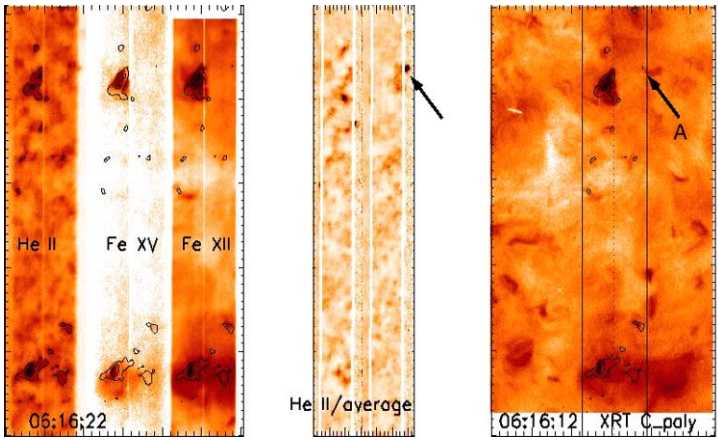

Figure 4 A frame from the movie showing the relationship between He II, Fe XV, Fe XII, and He II line shifts and X-ray emission from a region of quiet Sun on 7 November 2007. The left panel shows He II, Fe XV, and Fe XII EIS wide-slit images from two raster positions patched together, as linearly scaled negatives with contours of bright He II emission overlaid. The center panel shows the two neighboring He II images divided by their average He II image for the period. Here, the windows are not patched together so that emission changes beyond the image edge along the center line can be seen. Doppler shift events show up as black regions beyond the image edges, which are marked by solid white lines. An arrow points to a Doppler shift event near X-ray loop A. The right panel shows the closest in time XRT image with He II contours overlaid.

wide-slit positions, separated by 40 arcsec, were alternated, giving an 80-arcsec image every 1.5 min. The closest XRT C-poly image is placed alongside with He II contours overlaid. It is striking how often bright He II is found near the edge (footpoints) of X-ray structures. One good example is the structure marked A on Figure 4, where some of the strongest He II shifts were seen. In general the Fe XII and X-ray emissions correlate well.

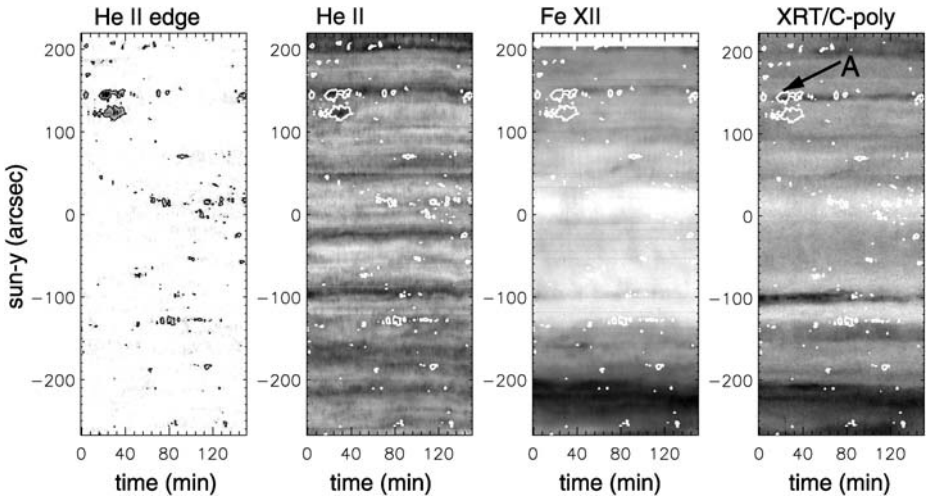

Figure 5 Time series of (a) He II intensity beyond the west edge of the image (blue shifts), (b) He II and (c) Fe XII intensity at the west edge, and (d) X-ray intensity at the position of the west edge. The contours outline positions of He II intensity beyond the image edge. In (a) darkness indicates the increase in blue wing intensity above the average for that position along the slit; (b) and (c) are linearly scaled intensity negatives and (d) is a logarithmically scaled intensity negative. The time is minutes after 06:05:16 UT on 7 November 2007.

Time series of emission beyond the image edge of He II and just inside He II and Fe XII images are shown in Figure 5 alongside the X-ray emission from the position of the images' edge. Any He II emission seen off the main image is produced by Doppler shifts from a region inside the image, so this directly compares He II shifts with the He II intensity and hotter plasma (Fe XII and X-ray) emission. The He II is reminiscent of explosive event distributions, where there are preferred event sites along network lanes spaced 50 – 100 arcsec apart, with events lasting 2 – 3 min, sometimes seen in bursts of up to 30 min (Innes *et al.*, 1997a; Innes, 2001). He II shifts seem to occur more frequently near sites of enhanced Fe XII and X-ray emission.

3.2. High Doppler Shifts near X-ray Spot Brightening

This observation, illustrated in Figures 6 and 7, is very unusual because the edge of the wide slit caught the brightening of an intense X-ray spot. Figures 6a – 6c show the time sequence of X-ray images. The X-ray brightening lasts less than 7 min. Simultaneously, there is a horizontal streak in all transition region and lower coronal line images with a length corresponding to a line width of 220 km s^{-1} beyond the window edge (Figure 7). There is no signature in the EIS coronal lines Fe XV and Fe XII.

The hot spot seems to be coming from the top of a cool loop seen faintly in the Si VII and Mg VII images. The images in the hotter lines, Fe XV and Fe XII, and the blends in He II suggest that one end of the cool coronal loop is rooted in a bright point and the other in the quiet Sun. The event lasted 1.5 min in Si VII and Mg VII and continued for another 3.5 min in the cooler He II line. At first glance the structure has the classic configuration of a reconnection jet above a coronal loop (*cf.* Hirayama, 1974; Kopp and Pneuman, 1976).

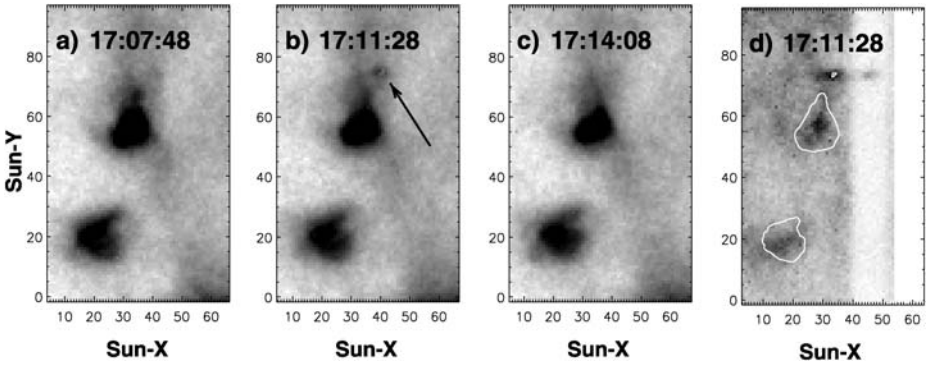

Figure 6 (a)–(c) Time series of XRT Al-mesh intensity showing hot spot brightening (indicated with an arrow) and (d) the EIS Si VII image with XRT contours on 10 April 2007. All intensities are represented as logarithmically scaled negatives.

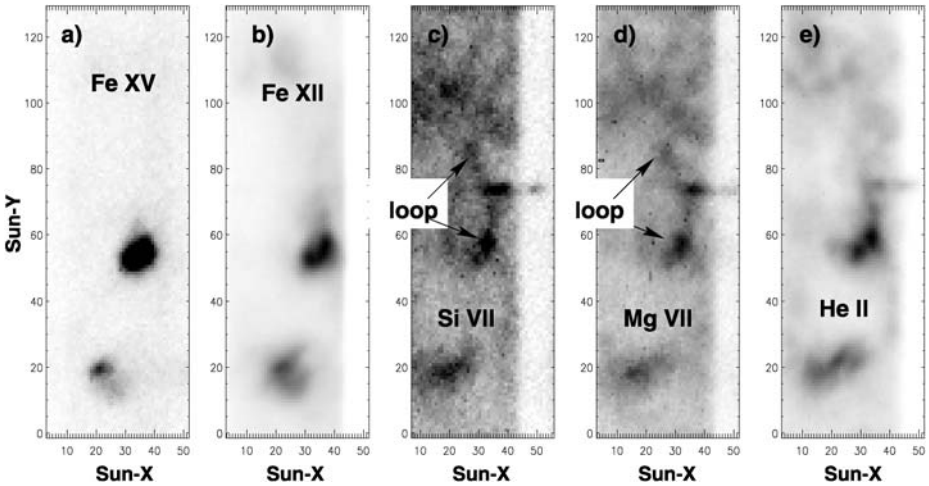

Figure 7 Upper transition region plasmoid or jet seen at 17:11:15 UT on 10 April 2007. The strong blue shift event is seen on the right-hand side of Si VII 275.35 Å, Mg VII 278.44 Å, and He II. All spectral images show blue shifts on the right and are represented as linearly scaled negatives.

3.3. Fe XV Doppler Shift

Shifts in coronal lines with formation temperature of about 2×10^6 K are also occasionally seen from X-ray structures. One example of a hot Fe XV and Fe XIV blue shift of about 120 km s^{-1} is shown in Figure 8. The outflow comes from an almost horizontal X-ray structure connecting a small X-ray brightening to a larger, more persistent X-ray region. It could be flow along a hot loop connecting the two X-ray regions. The shifts last about 25 min, during which time the brightening was seen to flare up and fade. The shift is also seen in Fe XII over a shorter period of time and with lower velocity.

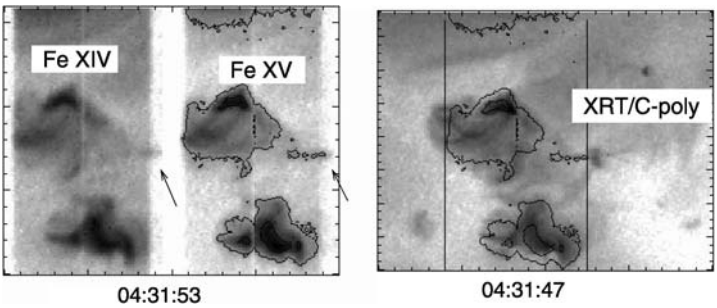

Figure 8 Example of Doppler shift seen in coronal lines on 15 November 2007. The images, from left to right, are EIS Fe XIV, Fe XV, and XRT C-poly. Arrows point to Doppler shifts seen beyond the image edge. The EIS image edges are indicated with solid lines in the XRT image. The contours outline the enhanced Fe XV emission.

4. Discussion

There is a wealth of information in the EIS 40-arcsec wide-slit images. The primary use of wide-slit images is to see rapid time variations of structures in specific spectral lines (Hansteen *et al.*, 2007), typically with a cadence 20 times (the slit width) faster than rastering with the 2-arcsec slit. After passing through the slit, the light is dispersed, producing rows of overlapping spectral images. If a Doppler shift occurs in the center of the image, this is indistinguishable from a horizontal structure. It is therefore beneficial to have simultaneous filtergrams to show the underlying structures.

Here we show how the wide slit can be used to detect Doppler shifts at the edge of the image. We have highlighted three types of Doppler-shift events seen in EIS wide-slit spectra: explosive events in He II at the image edge, a fast jet related to an X-ray spot brightening, and Fe XV flow connecting an X-ray spot brightening to a larger X-ray region. The latter observations were done in sit-and-stare mode at two positions spaced 40 arcsec apart to pick up first the blue and then the red wings of the lines. At present our understanding of the line profile at the edge of the slit is not sufficiently well understood to determine accurate line shifts, but flows producing emission more than two pixels away from the average line profile at the edge are clearly detectable.

This suggests new ways of investigating, for example, explosive event dynamics because one can see the loop motion and heating beyond the position of the explosive event. It could also be useful when investigating Doppler-shift fluctuations from hot loops because narrow-slit observations in sit-and-stare mode are unable to distinguish real intensity fluctuations at a point from movement of loops into and out of the slit field of view (*cf.* Wang *et al.*, 2003; Mariska *et al.*, 2007).

The aim of this short paper is to show the possibilities for future studies, not to present event details and their scientific implications. Discussions on the events themselves, including detailed analyses from SOT on *Hinode* and SUMER on SOHO, will be given in more extensive papers.

Acknowledgements We would like to thank Khalid Al-Janabi for his help with the EIS studies. Also many thanks are owed to the referee for constructive comments. *Hinode* is a Japanese mission developed and launched by ISAS/JAXA, collaborating with NAOJ as domestic partner and NASA (USA) and STFC (UK) as international partners. Scientific operation of the *Hinode* mission is conducted by the *Hinode* science team organized at ISAS/JAXA. Support for the postlaunch operation is provided by JAXA and NAOJ, STFC, NASA, ESA (European Space Agency), and NSC (Norway). We are grateful to all teams for their efforts in the design, building, and operation of the *Hinode* and SOHO missions.

References

Brueckner, G.E., Bartoe, J.D.F.: 1983, *Astrophys. J.* **272**, 329.
Chae, J., Wang, H., Lee, C., Goode, P.R., Schühle, U.: 1998, *Astrophys. J.* **504**, L123.
Culhane, J.L., Harra, L.K., James, A.M., Al-Janabi, K., Bradley, L.J., Chaudry, R.A., *et al.*: 2007, *Solar Phys.* **243**, 19.
Dere, K.P., Bartoe, J.D.F., Brueckner, G.E.: 1989, *Solar Phys.* **123**, 41.
Golub, L., Deluca, E., Austin, G., Bookbinder, J., Caldwell, D., Cheimets, P., *et al.*: 2007, *Solar Phys.* **243**, 63.
Hansteen, V.H., de Pontieu, B., Carlsson, M., McIntosh, S., Watanabe, T., Warren, H.P., *et al.*: 2007, *Publ. Astron. Soc. Japan* **59**, 699.
Hirayama, T.: 1974, *Solar Phys.* **34**, 323.
Innes, D.E.: 2001, *Astron. Astrophys.* **378**, 1067.
Innes, D.E., Brekke, P., Germerott, D., Wilhelm, K.: 1997a, *Solar Phys.* **175**, 341.
Innes, D.E., Inhester, B., Axford, W.I., Wilhelm, K.: 1997b, *Nature* **386**, 811.
Kopp, R.A., Pneuman, G.W.: 1976, *Solar Phys.* **50**, 85.
Mariska, J.T., Warren, H.P., Ugarte-Urra, I., Brooks, D.H., Williams, D.R., Hara, H.: 2007, *Publ. Astron. Soc. Japan* **59**, 713.
Ning, Z., Innes, D.E., Solanki, S.K.: 2004, *Astron. Astrophys.* **419**, 1141.
Tsuneta, S., Ichimoto, K., Katsukawa, Y., Nagata, S., Otsubo, M., Shimizu, T., *et al.*: 2008, *Solar Phys.* **249**, 167.
Wang, T.J., Solanki, S.K., Innes, D.E., Curdt, W., Marsch, E.: 2003, *Astron. Astrophys.* **402**, L17.
Wilhelm, K., Curdt, W., Marsch, E., Schühle, U., Lemaire, P., Gabriel, A., *et al.*: 1995, *Solar Phys.* **162**, 189.
Wilhelm, K., Innes, E.E., Curdt, W., Kliem, B., Brekke, P.: 1998, In: Guyenne, T.D. (ed.) *Solar Jets and Coronal Plumes*, *ESA SP-421*, 103.
Winebarger, A.R., Emslie, A.G., Mariska, J.T., Warren, H.P.: 2002, *Astrophys. J.* **565**, 1298.
Young, P.R., Del Zanna, G., Mason, H.E., Dere, K.P., Landi, E., Landini, M., *et al.*: 2007a, *Publ. Astron. Soc. Japan* **59**, 857.
Young, P.R., Del Zanna, G., Mason, H.E., Doschek, G.A., Culhane, J.L., Hara, H.: 2007b, *Publ. Astron. Soc. Japan* **59**, 751.